



Drilling of nodular cast iron with a novel SiO₂ coating deposited by sol-gel process in HSS drill

Natália Fernanda Santos Pereira¹ · Juan Carlos Campos Rubio² · Anderson Júnior dos Santos² · Manuel Houmard³ · Marcelo Araújo Câmara² · Alessandro Roger Rodrigues⁴

Received: 19 June 2019 / Accepted: 16 September 2019 / Published online: 16 November 2019
© Springer-Verlag London Ltd., part of Springer Nature 2019

Abstract

The present study proposes a novel coating applied on high-speed steel (HSS) drills, thinner and less expensive than the commercial ones. This new coating consists in a silicon dioxide (SiO₂) deposited by sol-gel process, and its performance was studied by means of drilling tests in nodular cast iron. For comparison purposes, two other cutting tools were also evaluated: uncoated and TiN-coated by physical vapor deposition process. Four outputs were investigated: thrust force, hole average surface roughness, hole average diameter (D_A), and tool wear (VB_{Bmax}). Analysis of variance (ANOVA) was applied to determine the influences of the coatings and drilling parameters on the cutting performances. The results indicated that the SiO₂ coating achieved performances significantly superior to the uncoated tools. They also behaved close to the commercial TiN coating in some aspects. Scanning electron microscopy (SEM) analysis showed predominant flank wear in all the uncoated and coated tools. The “number of holes/maximum flank wear (VB_{Bmax})” ratios were calculated, indicating a performance 315% better for the SiO₂-coated tool when compared to the uncoated one. Therefore, the deposition of SiO₂ by sol-gel method is a promising technique to coat rapidly and efficiently cutting tools, including for tools of complex geometries such as drills.

Keywords Drilling · Sol-gel · SiO₂ · Coating · High-speed steel · Cast iron

1 Introduction

In the past few years, new wear-resistant coatings have been developed due to the necessary improvement of machining technology. Researchers and industries aim for higher cutting speed, better quality of the machined surface, and lower consumption of lubricants and coolants [1]. There are several

techniques for the deposition of coatings on metals, such as the physical vapor deposition (PVD), chemical vapor deposition (CVD), electrochemical deposition, plasma spraying, and sol-gel process [2]. About this last technology, the process consists in the solidification of a sol in gel, where the sol is a dispersion of colloidal particles (1–100 nm) in a liquid, and a gel is an interconnected rigid network with pores of sub-micron dimensions and polymeric chain [3].

The sol-gel method stands out from conventional techniques because it is simple and less expensive and allows the coating of complex geometries [4]. Moreover, the deposition of thin homogeneous inorganic films by the sol-gel technique is reproducible in large scales and applicable to various types of substrates [5]. The sol-gel coating method does not involve the vacuum phase, requires low processing temperature, and can achieve a high degree of purity in oxide coatings [5, 6]. The applications for sol-gel coatings include anti-corrosion coatings, optical sensors, and, more recently, as thermal barriers or high electrochemical performance films [7, 8].

Although the coatings obtained by the sol-gel technique are little exploited in cutting tools, relevant studies have been carried out. Huang et al. [9] used the sol-gel

✉ Natália Fernanda Santos Pereira
nataliapereira@asesi.edu.br

¹ Department of Production Engineering, Federal University of Minas Gerais, Av. Presidente Antônio Carlos, 6627, Belo Horizonte, CEP 31270-901, Brazil

² Department of Mechanical Engineering, Federal University of Minas Gerais, Av. Presidente Antônio Carlos, 6627, Belo Horizonte, CEP 31270-901, Brazil

³ Department of Materials and Construction Engineering, Federal University of Minas Gerais, Av. Presidente Antônio Carlos, 6627, Belo Horizonte, CEP 31270-901, Brazil

⁴ Department of Mechanical Engineering, University of São Paulo, Av. Trabalhador São-Carlense, 400, São Carlos, CEP 13566-590, Brazil

method to coat two types of carbide powders, TiC and (W,Ti)C, with an alumina film. The new tool materials presented considerably improved fracture toughness compared to other ceramic tool materials. Machining tests showed that the new tool materials had superior wear resistance along with the other ceramics and could maintain a suitable wear resistance over the entire tool life. In another study, Tlili et al. [5] analyzed the wear behavior of alumina sol-gel coatings deposited on stainless steel. The alumina layers improved the tribological behavior of stainless steel and reduced wear and damages. Finally, Rubio et al. [10] evaluated the performance of TiO₂-coated tools by analyzing thrust force, burr height, and the maximum diameter when drilling aluminum sandwich material. The drilling tests were carried out using sol-gel coated high-speed steel (HSS) drills. The coated tool exhibited the best performance and improved the holes' quality. The coating seemed to decrease the maximum diameter of the hole, avoiding the formation of build-up-edge of aluminum due to a lower friction coefficient.

In addition to the sol-gel coatings aforementioned, coatings of silicon dioxide (SiO₂) can also be obtained by this technique. The SiO₂ coating presents excellent chemical stability, low thermal expansion, mechanical durability, and effective protection to metallic substrates [2, 7, 11]. In their research, Vasconcelos et al. [7] developed a SiO₂ coating on an AISI 304 stainless steel. The authors confirmed that a thin SiO₂ layer improved the anti-corrosion performance of the substrate used. HSS drills are widely used because of their low cost and high toughness in relation to the carbide ones, and no study was found regarding the use of sol-gel SiO₂-coating on this type of cutting tool. Additionally, this coating is compared with commercially available TiN-coated via PVD.

The PVD coating method was originally developed for HSS coating, whose material structure can be thermally influenced at high temperatures. While the CVD is performed in the range of 1000–1200 °C, the PVD uses lower temperatures (< 500 °C) [12]. Since the sol-gel coating is processed at low temperatures, it may be a promising method for coating HSS tools.

In this context, the present research evaluates the efficiency of the sol-gel method as a coating technique for HSS tools. To this purpose, we assessed the drilling process and tool wear during the drilling of nodular cast iron in three twist drills: uncoated, SiO₂-coated by sol-gel method, and TiN-coated by the PVD process. The analysis of variance (ANOVA) was used to determine the influences of the coatings and drilling parameters on the cutting performances. The surface characteristics of the tools were analyzed to determine their wear nature by using scanning electron microscopy (SEM) and energy dispersive spectroscopy (EDS) techniques.

2 Materials and methods

2.1 Tools

Twist HSS drills type AISI M2 were adopted, with 10 mm diameter, 118° point angle, and a 20° helix angle. To guarantee the initial conditions of each test, a new tool was used in each run. The drills underwent the same process of sharpening and faceting before coating, as detailed in Fig. 1.

2.2 Coatings

The preparation of the SiO₂ coating solution consisted of mixing deionized water, ethanol (C₂H₅OH), and hydrochloric acid (HCl) with tetraethoxysilane (TEOS). In the prepared sol-gel solution, the concentration of silicon atoms corresponded to 2.35 mol/L; the pH was 3.5, and the water/TEOS ratio was 2.2, all in agreement with the study of Houmard et al. [13]. The solution was aged for 48 h at room temperature and diluted to reach 1.5 mol/L. Before the deposition process, the drills underwent ultrasonic cleaning in ethanol.

Subsequently, the drills were coated by immersion (dip-coating) in the sol-gel solution with a withdrawal speed of 0.5 mm/s. The drills were covered with three coating layers, and after each layer, the coating was dried at 80 °C. At the end of the deposition process, the drills were heat-treated at 400 °C for 2 h to reduce the porosity, increase the density of the SiO₂ film and, thus, favor the coating resistance. The coated drills were then left to cool gradually inside the oven. Figure 2 shows a scheme of the dip-coating process performed in this research.

SiO₂- and TiN-coated tools were characterized, respectively, by using FEG 3D FEI and Jeol JSM-IT300 SEM microscopes both equipped with EDS. The friction coefficients were also measured by performing a pin-on-disc test method using a tribometer model Microtest SMT-A/0100.

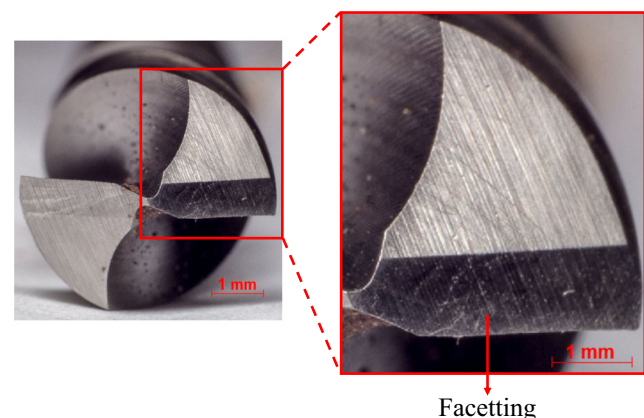


Fig. 1 Drill region with faceting

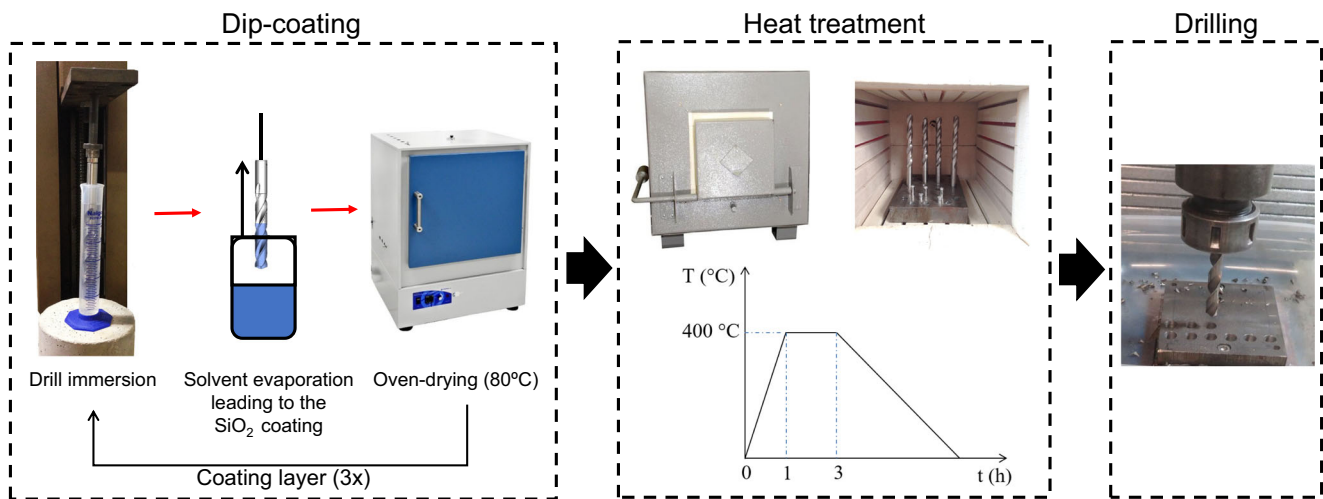


Fig. 2 Preparation steps of the SiO₂-coated drills by sol-gel technique

2.3 Workpiece

The material employed in the drilling tests was a FE42012 nodular cast iron with 110 mm × 120 mm cross-section area and 15-mm thickness. Three workpieces were used in drilling tests each one with a different tool. Chemical composition and mechanical properties of the nodular cast iron are summarized in Table 1.

2.4 Drilling experimental setup

Drilling experiments were carried out under dry condition on a machining center with 9.0-kW spindle power and a 7.500-rpm maximum spindle speed. Figure 3 shows the experimental drilling setup. Thrust force (F_z) was measured with a 4-component piezoelectric dynamometer 9272 Kistler, amplifier 5073 Kistler, and USB 6366 acquisition boards. The SignalExpress signal processing software by National Instrument was used by adopting an acquisition rate of 300 S/s (Samples per second).

Hole wall surface roughness was quantified using a portable Taylor Hobson Precision® roughness perthometer, model Surtronic 25, with a sample length of 2.5 mm and an evaluation length of 12.5 mm. Four measurements were taken for each hole in order to obtain a mean R_a . Furthermore, hole wall surface roughness was qualified by means of its topography (3D) and profile (2D) in axial direction. Thus, the profilometer

Table 1 Chemical composition and mechanical properties of the nodular cast iron used in the drilling tests

Fe	C	Si	Mn	P	S	Mg
93.68	3.63	2.47	0.09	0.06	0.01	0.06
Tensile strength (MPa)		Yield strength (MPa)		Elongation (%)		
554		376		14		

Hommelwerk T8000 and Hommelmap Expert 6.2 software were employed to obtain the images. This visual analysis was done for significant control factors, i.e., tool feed and drill coating (Table 5). As cutting speed was not significant, intermediate cutting speed of 55 m/min (Table 2) was considered in analysis of hole roughness.

Regarding hole diameter inspection, average diameters were measured using a coordinate measuring machine model Mitutoyo QM-Measure 353 with 0.5- μ m resolution. The final diameter presented in this paper corresponds to the average of three measurements taken at 4-mm, 8-mm, and 12-mm depth for each hole.

A full factorial experimental design was employed, and each drilling condition was replicated once, thus resulting in 54 runs. Table 2 presents the parameters or factor controls and their respective levels employed in the experimental work. The ranges of cutting parameters were selected based on the tool manufacturer recommendation and industrial applications.

Analysis of variance (ANOVA) was carried out, aimed to verify whether the main factors and their interactions are statistically significant within a 95% confidence interval. A p value (probability of significance) lower than or equal to $\alpha = 0.05$ indicates that the main factor or the interaction significantly affects the studied response.

2.5 Wear evaluation

Maximum flank wear (VB_{Bmax}) was measured by using SEM microscopy. For this purpose, the facetting region of the drill was measured before using an optical microscope (MO) Olympus SZ61 and after the drilling processes by SEM. The cutting conditions of 40 m/min cutting speed and 0.25 mm/rev feed were considered to tool wear analysis. These drilling test conditions were chosen because they are within the parameters recommended by the manufacturer. The surface

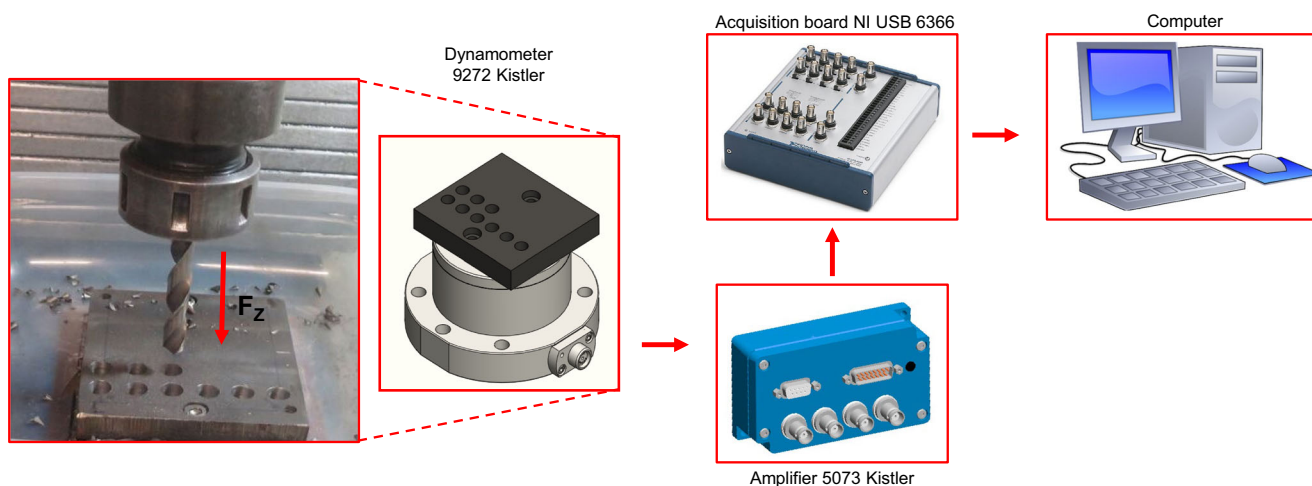


Fig. 3 Drilling experimental setup

morphology was studied after the drilling experiments by SEM and EDS. The drill end life criterion was defined when any of the following conditions have been reached: (i) the drills were not able to further cut properly and (ii) the drills showed the occurring of chipping in the flank region. The number of holes performed and the corresponding VBBmax were recorded for each tool after the wear test.

3 Results and discussion

3.1 Coating characterization

The final coating thickness ranged from 490 to 540 nm, as illustrated in the SEM micrograph of Fig. 4b. EDS surface analysis on the SiO₂ film confirmed the presence of Si and O elements, corresponding to the SiO₂ compound (Fig. 4a). Fe, Cr, and Mo present in the spectrum come from the substrate due to the high X-ray penetration depth. EDS analysis of the substrate (Fig. 4c) indicates the expected chemical elements of the HSS composition, i.e., Fe, W, Mo, Cr, and V.

Another coating tested in this study was the commercial TiN one deposited by the PVD process (TiN Balinit A from Balzers). The film was characterized by SEM and EDS, presenting thickness of about 3.7 to 3.9 μm (Fig. 5b). EDS analysis on coating indicates the presence of the Ti, N, and Fe. Mo,

Table 2 Drilling process parameters and their levels used during the experiments

Parameters/control factors	Levels		
	Uncoated	SiO ₂ coated	TiN coated
Tools, <i>T</i>			
Cutting speed, <i>v_c</i> (m/min)	40	55	70
Feed, <i>f</i> (mm/rev)	0.05	0.15	0.25

Cr, V, W, C, and Fe were identified on substrate, corresponding to the HSS material, as shown in Fig. 5a and c.

Table 3 presents the friction coefficient between the tribological pairs (workpiece material and drill coating/uncoating). The presence of coatings contributed to lower values of friction coefficient, i.e., SiO₂ coating reduced friction coefficient up to 55% while TiN one diminished up to 63% when compared to the uncoated drill. Emphasis must be given for 55 m/min cutting speed in which SiO₂ coating reaching the same friction coefficient from commercial TiN when considering measurement variability.

3.2 Drill performance

Table 4 shows the results of the thrust force (F_z), hole wall average roughness (R_a), and hole average diameter (D_A). *p*-values lower than 0.05 were underlined in Table 5 (ANOVA). R^2 values obtained in this study indicated that the statistical model adopted explains between 73 and 97% of the data.

3.3 Thrust force (F_z)

According to Table 5, tool and drill feed, as well as their interaction affect statistically the thrust force, respectively, with *p* values equal to 0.001, 0.001, and $0.013 < \alpha = 0.05$. Figure 6 shows the interaction of both parameters on the thrust force. TiN-coated tool presented lower values of thrust force and exhibited better performance. The thrust force for the SiO₂-coated tool was lower than for the uncoated tool and higher than for the TiN-coated tool. The presence of SiO₂ and TiN coatings reduced the friction and the contact area between the tool/chip and tool/workpiece interfaces probably due to their high heat resistance, as declared by Wang et al. [9, 14]. This fact led to smaller thrust forces. Correspondingly, the lower friction coefficient

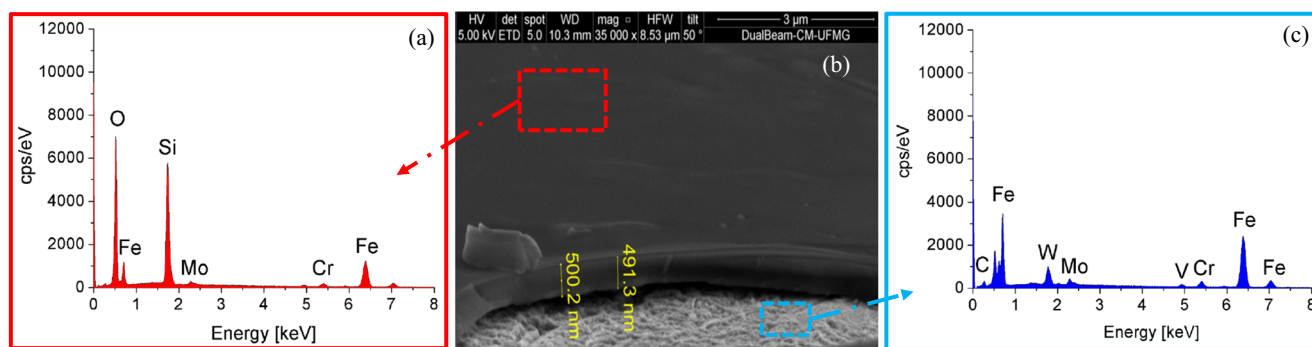


Fig. 4 **a** EDS spectrum from the drill coating, **b** SEM of the tool cross-section showing the SiO₂ film (some thickness measurements are indicated in the image), and **c** EDS spectrum from the substrate

values were obtained for the tribological pairs with SiO₂ and TiN coatings (Table 1). Regarding the effect of the feed, higher tool feeds remove more material amount per revolution increasing the thrust force. The increase of the feed results in higher areas at the primary and secondary zones. Consequently, chip section and thrust force increase significantly. Barbosa et al. [15] also observed thrust force increasing with tool feed in drilling tests. Finally, in agreement with Table 5, cutting speed does not influence the thrust force (p value = 0.062 > α = 0.05). Thus, the drill feed varies the thrust force more than tool (F -distribution = 477.67 \gg 17.62).

3.4 Surface roughness (R_a)

According to Table 5, tool and drill feed affected significantly the hole inner surface roughness (R_a), with p values, respectively, of 0.001, and 0.002 < α = 0.05. Figure 7 shows that higher feeds increase the average roughness and this behavior can be explained based on kinematic roughness, drill wear, and thrust force. Average or peak-to-valley roughness depends directly and quadratically on tool feed and inversely on drill corner radius [16]. Thus, the larger tool feed, the higher surface roughness. Besides, higher feeds create additional heat between the workpiece and the tool,

enhancing consequently the drill wear and leading to higher surface roughness [17]. As showed by Meena et al. [18], the increase in surface roughness with drill feed can be explained due to an increase in the chip section size. Khan et al. [19] have also reported a similar behavior when drilling AISI 1045 steel. As mentioned in Section 3.3, the thrust force increases when tool feed grows and hence poor surface finish is produced as a consequence. Under low feeds, hole inner average roughness decreases slightly for all drill evaluated.

The improvement in the hole inner surface quality due to the coating types is related to the coatings' effectiveness. Such films decrease the friction and tool-workpiece contact area resulting in better surface finish as a consequence. R_a values are within a range of 4.7 to 9.1 μm . A slight difference is observed for SiO₂ and TiN coatings (on average 0.8 μm). In addition, the coating deposited by the sol-gel method presented performance near TiN one for both thrust force and hole wall surface quality mainly for higher drill feeds.

The topography and profiles obtained by profilometry of the holes' inner surface are shown in Tables 6 and 7. Higher feed increases the average roughness observed by growing of the peak-to-valley distance regardless of tool tested. The topographies and profiles of the hole

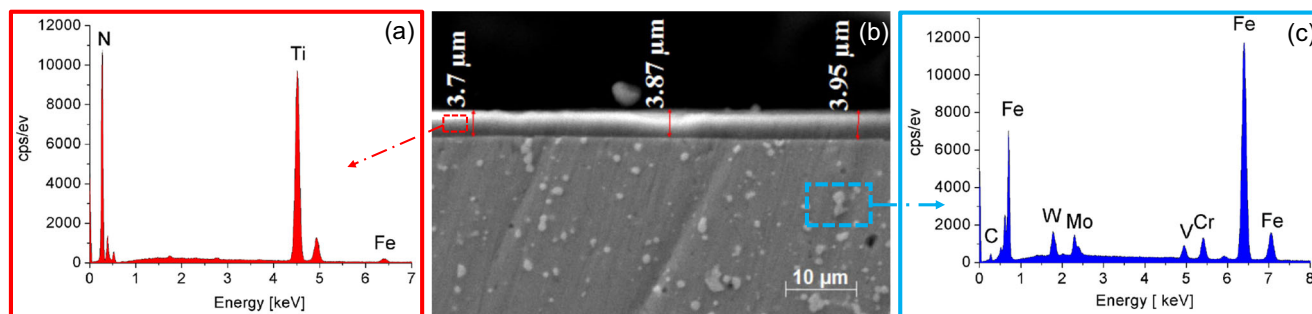


Fig. 5 **a** EDS drill spectrum from the coating, **b** SEM of the tool cross-section showing the TiN film (some thickness measurements are indicated in the image), and **c** EDS spectrum from the substrate

Table 3 Friction coefficient between the nodular cast iron disc and different coated pins

Cutting speed, v_c (m/min)	Uncoated	SiO ₂ coated	TiN coated
40	0.65 ± 0.05	0.40 ± 0.04	0.24 ± 0.02
55	0.73 ± 0.04	0.33 ± 0.04	0.28 ± 0.03
70	0.59 ± 0.05	0.47 ± 0.05	0.22 ± 0.02

wall surfaces obtained with coated tools demonstrate to be smoother than those attained with uncoated drill.

Figure 8 shows 2D profiles of the hole's inner surfaces drilled with SiO₂- and TiN-coated tool at 0.25 mm/rev feed. Similar microasperities' magnitudes were identified for these tool coatings and drill feed, which may justify the average roughness values (Fig. 7) very close for both tools. However, R_a amplitude parameter is neither capable of indicating untypical peaks or valleys nor defining the microirregularities' shapes,

although R_a is the most roughness amplitude parameter used for production control when machining with defined edge geometry cutting tools. In this context, statistical roughness parameters such as skewness (R_{sk}) and kurtosis (R_{ku}) are more suitable [20].

As seen in Fig. 8, R_{ku} for both tool coatings is lesser than 3.0, which means that both the texture features of the hole wall do not contain inordinately high peaks and/or deep valleys. Otherwise, R_{sk} is positive for SiO₂ and negative for TiN, indicating predominance of peaks and material concentration near machined surface, respectively.

According to Krolczyk et al. [20], R_{sk} parameter is useful in monitoring for different types of wear conditions and R_{ku} usually is employed to determine defects of peaks on working surfaces. Thus, these roughness parameters can be utilized to characterize tribological functionalities of parts working in contact.

Nodular cast iron is often used in powertrain systems, which comprises mechanical components like engines,

Table 4 Results for thrust force, hole wall average roughness, and hole average diameter

Tool, T	Cutting speed, v_c (m/min)	Feed, f (mm/rev)	Thrust force, F_z (N)		Average roughness, R_a (μ m)		Average diameter, D_A (mm)	
			Run	Replica	Run	Replica	Run	Replica
Uncoated	40	0.05	284.03	374.93	6.50	7.50	10.13	10.23
		0.15	498.03	636.40	7.10	8.40	10.10	10.13
		0.25	1030.23	1060.00	9.10	9.10	10.16	10.13
	55	0.05	385.32	432.76	7.60	8.10	10.08	10.19
		0.15	618.13	503.07	6.10	7.40	10.10	10.11
		0.25	1080.10	1095.00	6.90	9.00	10.11	10.06
	70	0.05	277.79	368.00	6.70	6.40	10.16	10.17
		0.15	506.53	633.40	8.20	6.10	10.15	10.16
		0.25	1206.10	1320.12	7.30	8.30	10.11	10.14
SiO ₂	40	0.05	191.38	281.42	6.70	5.70	10.11	10.16
		0.15	421.68	489.22	6.80	7.60	10.09	10.13
		0.25	1003.50	974.00	7.70	7.20	10.08	10.10
	55	0.05	380.12	419.95	6.10	6.30	10.10	10.14
		0.15	492.68	541.16	6.90	6.70	10.08	10.15
		0.25	1046.79	953.28	6.70	7.80	10.08	10.11
	70	0.05	227.74	388.78	6.60	6.00	10.21	10.13
		0.15	535.97	558.48	7.20	6.10	10.08	10.05
		0.25	939.00	820.00	7.00	7.50	10.09	10.11
TiN	40	0.05	233.11	317.09	4.70	5.00	10.05	10.08
		0.15	451.46	558.48	6.10	5.60	10.04	10.09
		0.25	758.65	870.17	7.00	7.20	10.07	10.06
	55	0.05	226.01	442.46	5.10	5.80	10.06	10.06
		0.15	454.58	471.90	5.90	5.10	10.03	10.04
		0.25	835.54	786.36	6.70	7.30	10.05	10.08
	70	0.05	258.05	344.80	6.40	5.30	10.06	10.16
		0.15	460.93	475.00	6.50	5.20	10.05	10.04
		0.25	1060.10	1001.42	6.60	6.00	10.04	10.06

Table 5 Results of the analysis of variance (ANOVA) over the thrust force, hole wall average roughness, and hole average diameter

Control factors	Thrust force, F_z (N)			Average roughness, R_a (μm)			Average diameter, D_A (mm)		
	SS ^a	F ^b	p value ^{c*}	SS	F	p value	SS	F	p value
Tool, T	156,428	17.62	<i>0.001</i>	221.137	25.1	<i>0.001</i>	0.0497	21.95	<i>0.000</i>
Cutting speed, v_c	27,438	3.09	0.062	0.9137	1.04	0.368	0.0034	1.53	0.236
Feed, f	4,241,487	477.67	<i>0.001</i>	139.215	15.8	<i>0.002</i>	0.0144	6.35	<i>0.005</i>
$T \times v_c$	25,930	1.46	0.242	11.433	0.65	0.633	0.0039	0.86	0.499
$T \times f$	69,119	3.89	<i>0.013</i>	10.219	0.58	0.680	0.0010	0.23	0.918
$v_c \times f$	46,653	2.63	0.057	19.285	1.09	0.379	0.0037	0.82	0.525
$T \times v_c \times f$	85,104	2.40	0.053	31.615	0.90	0.533	0.0079	0.88	0.546
R^2	97.49%			78.80%			73.36%		

^a Sum of squares (SS)

^b F -distribution (F)

^c Probability of significance (p value)

* p value in italic, significant values $< \alpha = 0.05$

transmissions, gears, bearings, and crankshafts [21]. Such pieces work under fluid-solid and/or solid-solid contact condition. Thereupon, SiO₂-coated drill yielded surface topography more indicated to retain fluid (fluid-solid interaction) and TiN-coated drill produced texture more appropriate to minimize wear (solid-solid contact).

3.5 Average diameter (D_A)

The tool and drill feed were significant over hole average diameter, with p values of 0.000 and $0.005 < \alpha = 0.05$, respectively (Table 5). The presence of coating contributed to minimize cutting stresses, which led to smaller dimensional variations. A similar result was found by Recep and Erdo [22] in which TiAlN-coated HSS tools showed lower diameter deviation than those for uncoated ones. Otherwise, the effect of

temperature rise contributed to increase the dimensional variations in dry machining. Rubio et al. [23] identified larger hole deformation for higher cutting temperatures in dry drilling. Thus, the dimensional variations were due to continuous rubbing of the drill and hot chips in the hole wall which leads to a workpiece expansion. This resulted in thermal distortion which in turn affected the hole accuracy. Therefore, ceramic coatings promoted a thermal barrier and contributed to smaller hole diameter deviations.

Figure 9 shows that higher feeds reduce the hole dimensional error, although thrust force and workpiece roughness are greater (Figs. 6 and 7). Lower tool feeds increase the friction which contributes to the larger dimensional variations. According to Table 4 and Fig. 9, SiO₂-coated drill minimized the holes' dimensional error

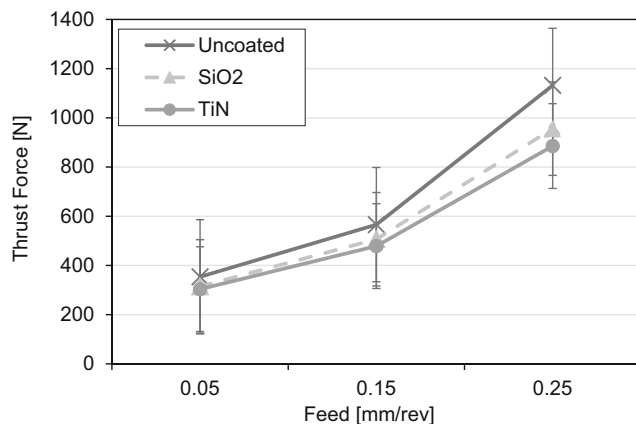


Fig. 6 Effect of drill feed and tool over the thrust force

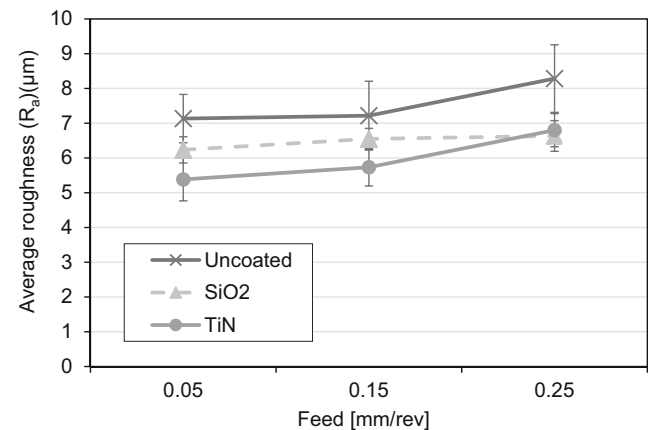
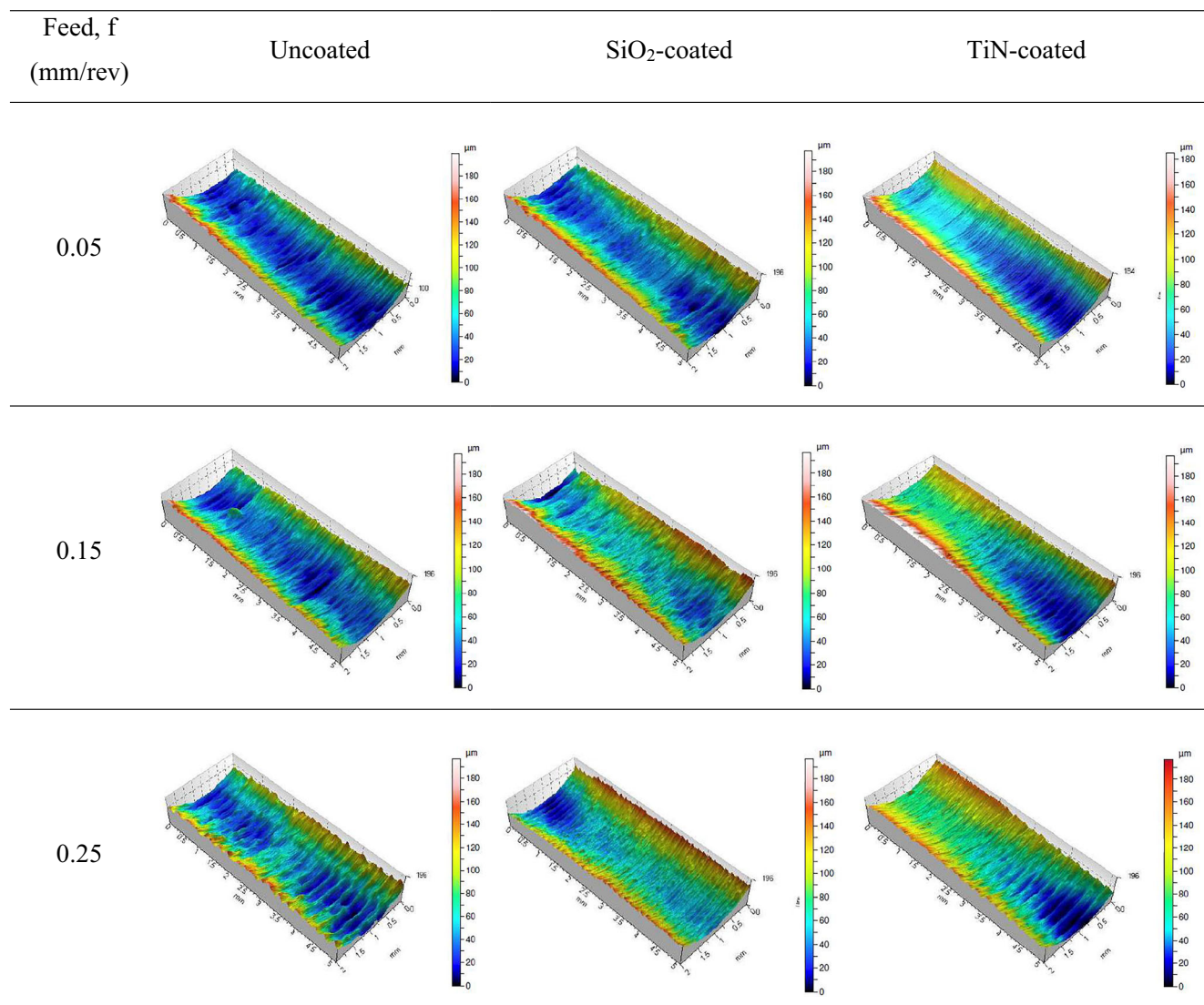


Fig. 7 Influence of the drill feed and tool on the hole wall average roughness (R_a)

Table 6 3D profilometry images of the holes' inner surface for 55 m/min cutting speed

by about 23 μm as compared with that for uncoated tool; however, TiN coating diminished in 72 μm on average this dimensional error. Furthermore, the dynamic instability and vibration during the drilling process play a crucial role in determining the hole quality [24]. Hence, stable drilling processes are demanded to produce holes with better quality in terms of lesser dimensional error and surface roughness.

3.6 Drill wear

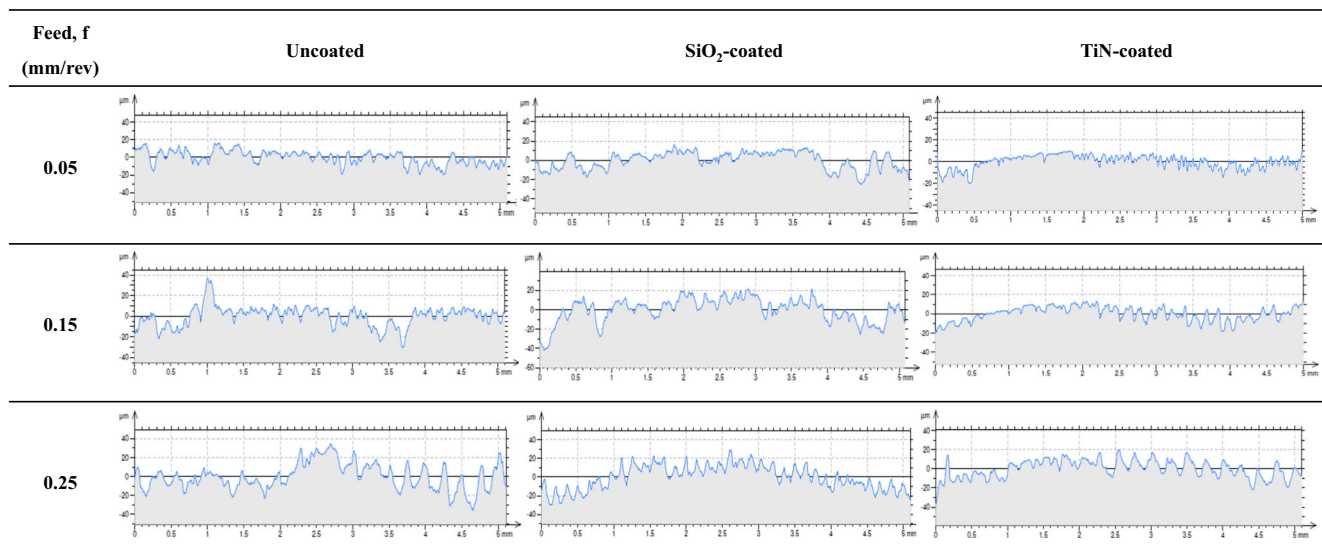
Drills' wear images are shown in Fig. 10 according to Section 2.5. The drills' faceting regions were considered as reference surface to measure the maximum flank wear. Only one drilling condition was taken into account to evaluate tool wear, i.e., 40 m/min cutting speed

and 0.25 mm/rev tool feed. All of three drills were examined. Figure 10 shows in upper line, MO images from drills' top view before wear while the bottom line presents SEM images after worn tools.

Some dimensions are displayed in Fig. 10 aiming at clearing the technique used to measure the drill wear. As an example, it seems that tool wear is identified and quantified according to flank wear progresses over faceting region. These measurements were done by using SEM microscopy given the larger resolution and magnification of images since the line between flank wear and faceting region could be difficult to define.

Figure 11 displays the number of holes and the $VB_{B\text{max}}$ of the corresponding tools. The graph shows that the highest values of $VB_{B\text{max}}$ were observed for the uncoated tool: 0.39 mm for 81 holes. SiO₂-coated tool presented a

Table 7 2D profilometry images of the holes’ inner surface for 55 m/min cutting speed



VB_{Bmax} of 0.31 mm, corresponding to 268 holes, and the TiN-coated drill reached 0.26 mm for 471 holes. The drilling lengths for the uncoated, SiO₂-coated, and TiN-coated tools were 1.215 m, 4.020 m, and 7.065 m, respectively.

In relation to the tool life, SiO₂- and TiN-coated drills outperformed the uncoated one by a factor of 3.3 and 5.8 times, respectively. These results are assigned to the thermal barrier promoted by the ceramic coatings due to their high heat resistance and their smaller friction coefficients.

For comparison, the number of holes in relation to the VB_{Bmax} was calculated for each tool. The “number of holes/VB_{Bmax}” ratio was 208 for the uncoated tool, 864 for the SiO₂-coated (+ 315%) and 1811 for the TiN-coated (+ 770%). SiO₂-coated tool presented a remarkable “number of holes/VB_{Bmax}” ratio when compared to the TiN-coated one, especially considering that the thickness of the SiO₂ coating is approximately six times lower than the TiN coating one. Thus, the SiO₂ coating performance can be considered absolutely satisfactory. Furthermore, the SiO₂ coating deposited by the sol-gel method presents the advantage of using a simple process which requires low processing temperature, and does not need the vacuum stage.

The surface characteristics of the tools were analyzed to determine the nature or mechanisms of wear, using SEM and EDS techniques (Fig. 12). Different tool damages were observed, including flank wear (especially at the outer corner of the drill), chipping (shown in the white circle in Fig. 12b, c), and apparent rounding at the main cutting edge.

The uncoated tool presented an accentuated flank wear and outer corner flank wear, with rounding at the main cutting edge (Fig. 12a). This drill exhibited a large amount of adhered material near the main and secondary cutting edges and at the side clearance surface. Flank wear was also observed in the SiO₂-coated tool, which presented adhered material in similar regions to the uncoated tool, visually in smaller proportions. This observation suggests that the coating could have been removed in the contact between the chip and workpiece surface after a certain number of drilled holes, which should in turn increase the friction and facilitate the adhesion. Indeed, it is known that multiple layers of chips are deposited along the tool during the drilling operation, and they are subsequently removed by abrasion, which can reduce the coating thickness at the same time [25]. Small chipping was observed in the main cutting edge of the SiO₂-coated tool (Fig. 12b).

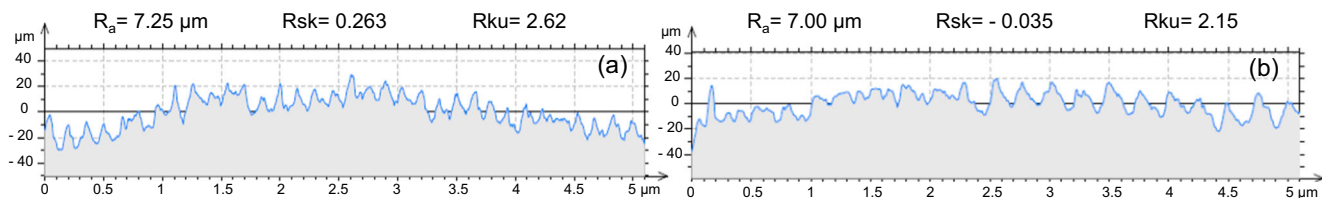


Fig. 8 2D profilometry images of the holes’ inner surface for 55 m/min cutting speed and 0.25 mm/rev feed with **a** SiO₂-coated and **b** TiN-coated drill

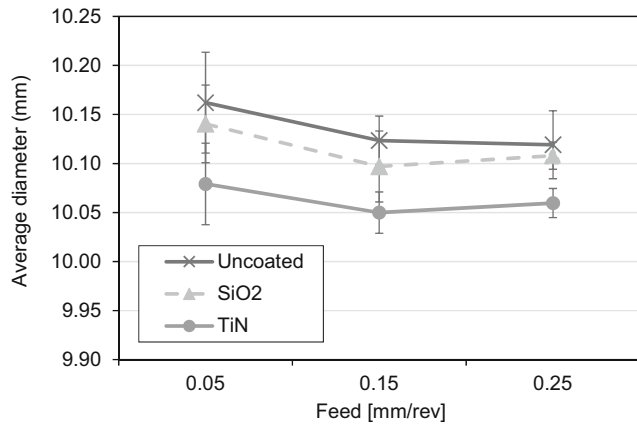


Fig. 9 Effect of drill feed and tool over the hole average diameter

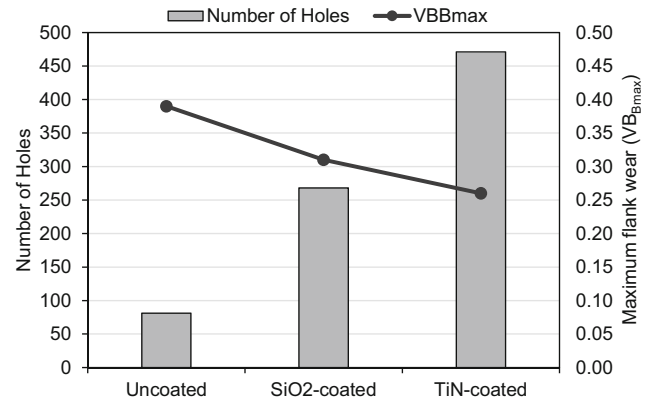


Fig. 11 Number of holes and maximum flank wear (VB_{Bmax}) of uncoated and coated tools

TiN-coated tool also presented flank wear and minor chipping. Adhered material was not found in the side clearance surface of the drill, which corroborates the findings of Hedenqvist et al. [14] when mentioning that TiN-coated tool could guarantee a shorter contact length between the tool and the workpiece resulting in a low adherence.

SEM images with higher magnification and the EDS spectra in the region of chipping shown in Fig. 13 suggest that the coatings were removed and the substrate of the HSS drills was exposed at the end of the drilling test. Adhered material and exposed substrate in the flank face can be explained by the contribution of the *attrition* wear mechanism.

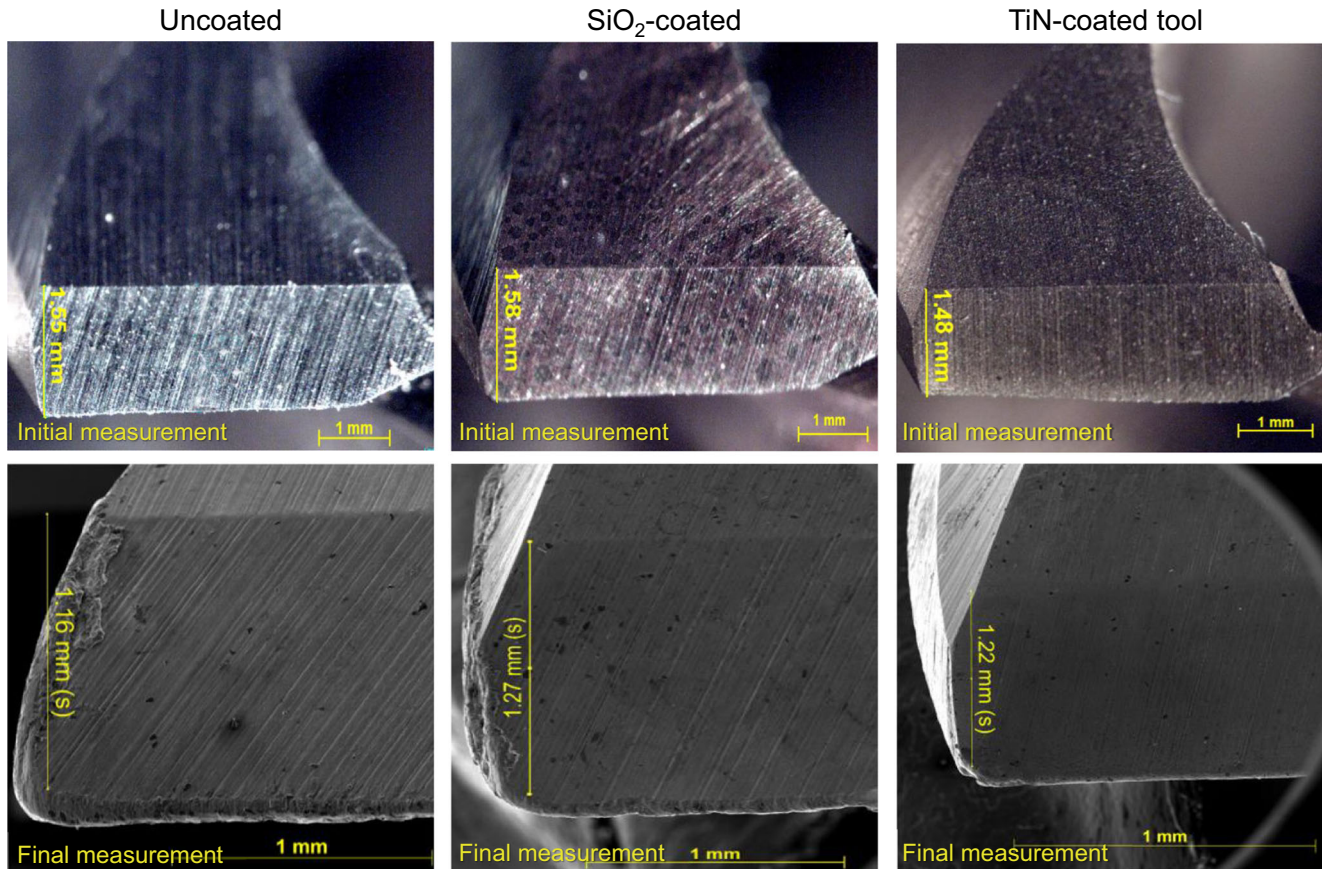


Fig. 10 Initial and final measurements in the evaluation of maximum flank wear (40 m/min cutting speed and 0.25 mm/rev tool feed)

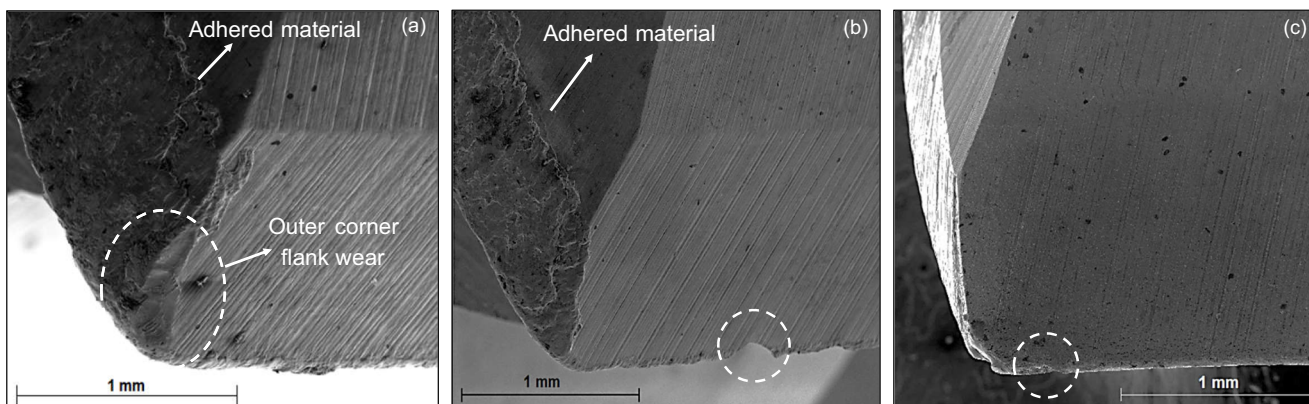


Fig. 12 SEM images of the drill surfaces: **a** uncoated tool, **b** SiO₂-coated tool, **c** TiN-coated tool. Chipping highlighted by white circles (**b** and **c**)

Similar results were found by Rosa et al. [26] in drilling tests using TiAlN-coated tools. The authors stated that the high normal pressure on the tool rake face, together with the vibration, may have occurred in the tool, leading to the extrusion of chips in the cutting edge. This effect induced the presence of adhered material in the worn area of the tool flank. The authors also reported that a relative movement between workpiece and tool takes place and generates a stick-slip process, which in turn removes particles from the tool (in a typical mechanism of *attrition*). Subsequently, the edge weakens because of the wear, and an increase in tool chipping follows consequently.

4 Conclusions

SiO₂-coated HSS drills were prepared using the sol-gel method and tested as for thrust force, hole inner surface roughness (R_a), hole mean diameter (D_A), and tool wear (VB_{Bmax}). The drilling results indicated that the SiO₂ coating achieved a performance significantly superior to the uncoated tool. They also behaved close to the commercial TiN coating per PVD process in some aspects. This result is assigned to the lower friction coefficient of ceramic-coated tools. Additionally, the SiO₂ coating presents a much more straightforward fabrication process and a thickness in the order of one-sixth of the TiN coating one.

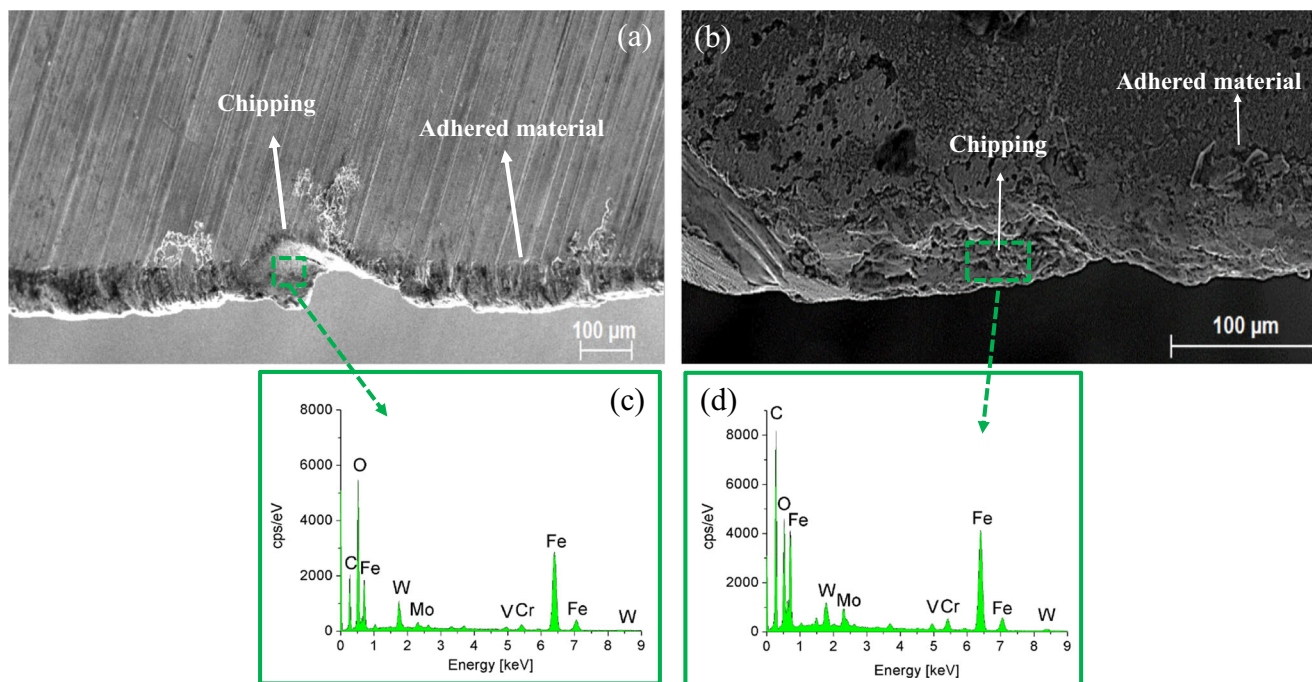


Fig. 13 SEM images of the drill flank faces: **a** SiO₂ coated tool and **b** TiN-coated tool. EDS spectra from **c** SiO₂-coated tool and **d** TiN-coated tool in the chipping regions

The main findings of this study can be summarized as follows:

- ANOVA indicated that the drill feed and type of tool significantly affected the thrust force. TiN tool obtained smaller thrust force in all tests; whereas the thrust force for the SiO₂-coated tool was lower than that of the uncoated tool. SiO₂ and TiN coatings contributed to a reduction of friction at the tool-chip and tool-workpiece interfaces given their high heat resistance, which in turn decreased the thrust force. On the other hand, as the drill feed increases the chip cross-section area enhances and the thrust force increases significantly for all of tools.
- Regarding the average roughness of the hole wall, the cutting tool presented significant influence by ANOVA. The highest values for R_a were obtained by the uncoated drill. The presence of coatings improves the hole quality, leading to lower R_a values. The increase in surface roughness as tool feed grows can be explained by larger chip cross-section area. The hole inner surface profile and topography produced by uncoated and coated drills showed greater peak-to-valley distance when tool feed is augmented, evidencing deterioration on the hole surface quality.
- The hole average diameter is significantly affected by drill feed and type of tool. A smaller feed contributed to higher contact time tool-workpiece and thus increased dimensional variation. On the other hand, the coatings contributed to minimize cutting stresses, cutting temperature, and dimensional variations. Concerning SiO₂-coated tool, hole dimensional error was minimized around of 23 μm when compared to that produced by uncoated drill.
- Uncoated, SiO₂-coated, and TiN-coated tools exhibited maximum flank wear of 0.39 mm, 0.31 mm, and 0.26 mm, respectively. The “number of holes/maximum flank wear (VB_{Bmax})” ratios were calculated, indicating a performance 315% better for the SiO₂-coated tool when compared to the uncoated one.
- SEM analysis showed the presence of adhered material at the side clearance surface in uncoated and the SiO₂-coated tools. The flank wear was also evidenced in all tools. Minor chipping and adhered material are observed near the cutting edge to coated tools. SEM and EDS analyses suggested that the coating was removed and, consequently, the substrate of the HSS drill was exposed, indicating the participation of the *attrition* wear mechanism.

In summary, the SiO₂ coating presents competitive advantages and the sol-gel method arises as a promising technique to improve the performance of cutting tools. Among its advantages are the low cost of processing, low coating temperatures, and rapid and straightforward coating deposition, including in tools with complex geometries such as twist drills.

Funding information This study was partly financed by the Coordenação de Aperfeiçoamento de Pessoal de Nível Superior - Brasil (CAPES) - Finance Code 001. This study also received financial support from the agencies FAPEMIG (Fundação de Amparo à Pesquisa do Estado de Minas Gerais) and CNPq (Conselho Nacional de Desenvolvimento Científico e Tecnológico).

Compliance with ethical standards

Conflict of interest The authors declare that they have no conflict of interest.

References

1. Carvalho S, Parreira NMG, Silva MZ, Cavaleiro A, Rebouta L (2012) In-service behaviour of (Ti,Si,Al)N_x nanocomposite films. *Wear* 274–275:68–74. <https://doi.org/10.1016/j.wear.2011.08.018>
2. Wang DD, Bierwagen GP (2009) Sol-gel coatings on metals for corrosion protection. *Progr Org Coat* 64:327–338. <https://doi.org/10.1016/j.porgcoat.2008.08.010>
3. Singh LP, Bhattacharyya SK, Kumar R, Mishra G, Sharma U, Garima S, Ahalawat S (2014) Sol-gel processing of silica nanoparticles and their applications. *Adv Colloid Interface Sci* 214:17–37. <https://doi.org/10.1016/j.cis.2014.10.007>
4. Chen Y, Ai X, Huang C, Wang B (2000) Preparation of α -alumina coated carbide tools by the sol-gel process. *Mat Sci Eng* 288:19–25. [https://doi.org/10.1016/S0921-5093\(00\)00840-6](https://doi.org/10.1016/S0921-5093(00)00840-6)
5. Tlili B, Barkaoui A, Walock M (2016) Tribology and wear resistance of the stainless steel. The sol-gel coating impact on the friction and damage. *Tribol Int* 102:348–354. <https://doi.org/10.1016/j.triboint.2016.06.004>
6. Bechinger C, Muffler H, Schäfle C, Sundberg O, Leiderer P (2000) Submicron metal oxide structures by a sol-gel process on patterned substrates. *Thin Solid Films* 366:135–138. [https://doi.org/10.1016/S0040-6090\(00\)00865-8](https://doi.org/10.1016/S0040-6090(00)00865-8)
7. Vasconcelos DCL, Carvalho JAN, Mantel M, Vasconcelos WL (2000) Corrosion resistance of stainless steel coated with sol-gel silica. *J Non-Cryst Solids* 273:135–139. [https://doi.org/10.1016/S0022-3093\(00\)00155-1](https://doi.org/10.1016/S0022-3093(00)00155-1)
8. Fenech J, Dalbin M, Barnabe A, Bonino JP, Ansart F (2011) Sol-gel processing and characterization of (RE-Y)-zirconia powders for thermal barrier coatings. *Powder Technol* 208:480–487. <https://doi.org/10.1016/j.powtec.2010.08.046>
9. Huang CZ, Wang J, Ai X (2000) Development of new ceramic cutting tools with alumina coated carbide powders. *Int J Mach Tools Manuf* 40:823–832. [https://doi.org/10.1016/S0890-6955\(99\)00102-9](https://doi.org/10.1016/S0890-6955(99)00102-9)
10. Rubio JCC, Rezende BA, Vieira LMG, Houmard M (2017) Drilling of aluminium/PE sandwich material with a novel TiO₂-coated HSS drill deposited by sol-gel process. *Int J Adv Manuf Technol* 92: 1567–1577. <https://doi.org/10.1007/s00170-017-0138-z>
11. Kermadi S, Agoudjil N, Sali S, Boumaour M, Bourgeois S, Marco De Lucas MC (2014) Sol-gel synthesis of xTiO₂(100 - X)SiO₂

- nanocomposite thin films: structure, optical and antireflection properties. *Thin Solid Films* 564:170–178. <https://doi.org/10.1016/j.tsf.2014.05.068>
12. Mrkvica I, Neslušan M, Čep R, Sléha V (2016) Properties and comparison of PVD coatings. *Teh. Vjesn. Tehnički vjesnik* 23(2): 569–574. <https://doi.org/10.17559/TV-20140509105317>
 13. Houmard M, Riassetto D, Roussel F, Bourgeois A, Berthomé G, Joud JC, Langlet M (2007) Morphology and natural wettability properties of sol-gel derived TiO₂-SiO₂ composite thin films. *Appl Surf Sci* 254:1405–1414. <https://doi.org/10.1016/j.apsusc.2007.06.072>
 14. Hedenqvist PER, Olsson M, Wallen PER, Kassman ASA, Hogmark S (1990) How TiN coatings improve the performance of high. *Surf Coat Technol* 41:243–256
 15. Barbosa PA, Costa ES, Guesser WL, Machado AR (2014) Comparative study of the machinability of austempered and pearlitic ductile irons in drilling process. *J Braz Soc Mech Sci Eng* 37: 115–122. <https://doi.org/10.1007/s40430-014-0161-z>
 16. Shaw MC (2005) *Metal cutting principles*. Oxford University Press, New York
 17. Ankalagi S, Gaitonde VN, Petkar P (2017) Experimental studies on hole quality in drilling of SA182 steel. *Materials today: proceedings* 4(10):11201–11209. <https://doi.org/10.1016/j.matpr.2017.09.041>
 18. Meena A, El Mansori M (2013) Specific cutting force, tool wear and chip morphology characteristics during dry drilling of austempered ductile iron (ADI). *Int J Adv Manuf Technol* 69: 2833–2841. <https://doi.org/10.1007/s00170-013-5220-6>
 19. Khan SA, Nazir A, Mughal MP, Saleem MQ, Hussain A, Ghulam Z (2017) Deep hole drilling of AISI 1045 via high-speed steel twist drills: evaluation of tool wear and hole quality. *Int J Adv Manuf Technol* 93:1115–1125. <https://doi.org/10.1007/s00170-017-0587-4>
 20. Krolczyk GM, Maruda RW, Krolczyk JB, Nieslony P, Wojciechowski S, Legutko S (2018) Parametric and nonparametric description of the surface topography in the dry and MQCL cutting conditions. *Measurement* 121:225–239. <https://doi.org/10.1016/j.measurement.2018.02.052>
 21. Ceschini L, Campana G, Pagano N, Angelini V (2016) Effect of laser surface treatment on the dry sliding behaviour of the ENGJS400-12 ductile cast iron. *Tribology International* 104:342–351. <https://doi.org/10.1016/j.triboint.2016.09.018>
 22. Recep B, Erdo T (2017) Investigation of the effects of cutting parameters on diameter deviation in drilling of HSLA steel. *Turk J Electromech Energy* 2:3–8
 23. Rubio JCC, Rezende BA, Vieira LMG, Romero HM, Brenes LAR (2019) Comparative study on lubricating and cooling conditions in the drilling process of electrolytic copper. *Int J Adv Manuf Technol* 101:2633–2641. <https://doi.org/10.1007/s00170-018-3139-7>
 24. Kaplan Y, Motorcu AR, Nalbant M, Okay Ş (2015) The effects of process parameters on acceleration amplitude in the drilling of cold work tool steels. *Int J Adv Manuf Technol* 80:1387–1401. <https://doi.org/10.1007/s00170-015-7097-z>
 25. Cardoso MJ, Polli ML, Pintaude G (2018) Wear analysis of PVD-coated twist drills under MQL. *Ind Lubr Tribol* 70(9):1664–1669. <https://doi.org/10.1108/ILT-10-2016-0243>
 26. Rosa N, Diniz AE, Neves D, Salles BB, Guerreiro SS (2014) Analysis of the life of cemented carbide drills with modified surfaces. *Int J Adv Manuf Technol* 71:2125–2136. <https://doi.org/10.1007/s00170-013-5598-1>

Publisher's note Springer Nature remains neutral with regard to jurisdictional claims in published maps and institutional affiliations.